

Different Features of Jets and Isotropic Fireballs in Gamma-ray Burst Phase *

Yun-Ming Dong, Lan-Wei Jia and Xiao-Hong Zhao

Yunnan Astronomical Observatory/National Astronomical Observatories, Chinese Academy of Sciences, Kunming 650011; dongym@ynao.ac.cn
Graduate University of Chinese Academy of Sciences, Beijing 100049

Received 2005 June 20; accepted 2005 October 27

Abstract We investigated physical quantities including the spectrum, emission lines and pulse profiles expected from a uniform jet, a spherical fireball and the $1/\Gamma$ region (the portion of the spherical fireball with opening angle $1/\Gamma$) in the prompt emission phase, after taking into consideration of the Doppler effect under the fireball framework. Our study shows that: a) for these physical quantities the spherical fireball and the uniform jets do not present obvious differences, so we cannot use these to distinguish a spherical fireball from a uniform jet; b) for the spherical fireball and a uniform jet, the observed quantities mainly come from the $1/\Gamma$ region, so we can simply use the $1/\Gamma$ region in approximate calculations; c) broadening of emission lines is a general phenomena, which mainly comes from the curvature effect; d) the $1/\Gamma$ region plays different roles in different frequency ranges, and the radiation from the $1/\Gamma$ region is greater in the higher than in the lower frequencies.

Key words: gamma-rays: bursts—gamma-rays: theory—radiation mechanisms: non-thermal —relativity

1 INTRODUCTION

The fireball shock model is a main and generic theoretical model which is widely used to interpret the current gamma-ray bursts (GRBs) and afterglow observations (see, e.g., Zhang & Mészáros 2003; Piran 1999, 2004; Mészáros 2002; Cheng & Lu 2001). Due to the observed great output rate of radiation, in the context of cosmological origin, the fireball should be expanding relativistically (Paczynski 1986; Goodman 1986), which has been further corroborated by the radio afterglow data that initially show large interstellar scintillation (Waxman, Kulkarni & Frail 1998) and the analysis of early afterglow reverse shock data (Sari & Piran 1999; Zhang, Kobayashi & Mészáros 2003). For most gamma-ray bursts, the typical Lorentz factor is $\Gamma \sim 100 - 1000$. Thus, the Doppler effect must be at work (Mészáros & Rees 1998).

It is widely accepted today that many GRBs are beamed (Rhoads 1997, 1999; Panaitescu, Mészáros & Rees 1998; Panaitescu & Kumar 2001; Sari & Piran 1999; Frail et al. 2001; Dai & Cheng 2001; Dai et al. 2001; Huang et al. 2002; Zhang & Mészáros 2002; Wei & Jin 2003). The GRB jet is originally thought to be a uniform jet (UJ) not containing any structures (Rhoads 1997; Sari, Piran & Halpern 1999). The character of the uniform jet is that all the parameters (density n , Lorentz factor Γ , magnetic and electron equipartition factors ϵ_B and ϵ_e , etc.) are constants throughout the jet. Later, authors have found that the GRB jet perhaps has a complicated configuration. There are two main GRB jet structure models which are currently under debate. One is the universal

* Supported by the National Natural Science Foundation of China.

structured jet (USJ) model suggested by Rossi, Lazzati & Rees (2002) and Zhang & Mészáros (2002), in which parameters such as the emitted energy (ϵ) varies as a function of the angle from the jet axis. The other is two-component jet model (Berger et al. 2003; Huang et al. 2004). The opening angle (UJ model) or the viewing angle (USJ model) of the jet (θ_{jet}) can be calculated from the sharp breaks and/or quick decays observed in the afterglow light curves (Phoads 1997; Sari et al. 1999). From Table 1 of Friedman & Bloom (2005), the smallest and the largest θ_{jet} of 52 well-studied GRB afterglows to date have been obtained as 3.24 and 22.95 degrees, respectively.

Table 1 List of ν_{line} and $\Delta \nu_{\text{FWHM}}/\nu_{\text{line}}$ for the Two Narrow Emission Lines

Γ	$\nu_{0,\text{line}}/\nu_{0,p}=0.01$		$\nu_{0,\text{line}}/\nu_{0,p}=100$	
	$\nu_{\text{line}}/\nu_{0,p}$	$\Delta \nu_{\text{FWHM}}/\nu_{\text{line}}$	$\nu_{\text{line}}/\nu_{0,p}$	$\Delta \nu_{\text{FWHM}}/\nu_{\text{line}}$
1×10^0	1.00×10^{-2}	2.46×10^{-2}	1×10^2	2.46×10^{-2}
1×10^1	1.95×10^{-1}	1.71×10^{-1}	1.95×10^3	1.71×10^{-1}
1×10^2	1.95×10^0	1.71×10^{-1}	1.95×10^4	1.71×10^{-1}
5×10^2	9.72×10^0	1.71×10^{-1}	9.72×10^4	1.71×10^{-1}

Note: for any given Γ , ν_{line} and $\Delta \nu_{\text{FWHM}}/\nu_{\text{line}}$ are actually the same for the spherical fireball, the $1/\Gamma$ region, and jets with half opening angles of 0.4, 0.228 and 0.056.

According to the relativistic radiation theory, in the prompt emission phase when the fireball has a highly relativistic bulk motion, the observed radiation should mainly come from a region with the opening angle $\theta \sim \Gamma^{-1}$ ($1/\Gamma$ region). Photons emitted from this narrow region can be detected by the observer: this is the relativistic beaming effect. For a typical Lorentz factor of 100, the opening angle of the $1/\Gamma$ region would be about 0.57 degree. The opening angle of the beaming region is far less than the smallest θ_{jet} in the prompt emission phase. Therefore, we will encounter two questions in the study of GRBs, one is whether we can use some prompt emission features to tell apart a spherical fireball from a jet, and the other is what role the $1/\Gamma$ region plays in the prompt emission phase. In this work, we will focus our attention to these issues.

Studies of the Doppler effect of the expanding fireball surface have been presented by different authors, and based on these studies formulas applicable to various situations were suggested (Fenimore et al. 1996; Granot et al. 1999; Eriksen & Gron 2000; Dado et al. 2002a, 2002b; Ryde & Petrosian 2002; Kocevski et al. 2003; Qin 2002). Qin (2002, 2003) and Qin et al. (2004) theoretically investigated the expected spectrum, emission lines and pulse of the light curves affected by the Doppler effect in the fireball framework for the isotropic spherical surface. They found that the shape of the expected spectrum remains almost the same as that of the corresponding rest frame spectrum for the constant radiations of the Bremsstrahlung, Comptonized, and synchrotron mechanisms as well as for that of the Band spectrum and the expansion speed of fireball is a fundamental factor of the enhancement of the flux of gamma-ray bursts. The spectral lines are strongly affected by the Doppler effect, and the narrow lines are broadened and the observed relative width would approach 0.162. The expected pulses of the light curves are similar for different local pulses. In this work, under the consideration of the Doppler effect, we followed the method of Qin (2002, 2003) and Qin et al. (2004) to investigate the expected spectrum, emission lines and pulse profiles resulting from the $1/\Gamma$ region, the spherical fireball and uniform jets with the smallest and the biggest θ_{jet} available, respectively, assuming the empirical spectral energy distribution form, known as the Band spectrum (Band et al. 1993).

This paper is organized as follows: In Section 2, we investigate the expected spectra from the $1/\Gamma$ region, the spherical fireball and the uniform jets with three different opening angles. The corresponding expected emission lines are investigated in Section 3. The expected pulses are presented in Section 4. Finally, a discussion and conclusions are presented.

2 THE EXPECTED SPECTRUM

The expected spectrum affected by the Doppler effect for the isotropic spherical fireball was obtained by Qin (2002). For constant radiation with a certain radiation mechanism in the rest frame,

the expression of the expected spectrum affected by the Doppler effect for the isotropic spherical fireball is described by

$$\nu f_\nu(t) = \frac{2\pi I_0 \tilde{R}^2(t) \nu}{D^2 \Gamma^3} \int_0^{\pi/2} \frac{g_{0,\nu}(\nu_{0,\theta}) \cos \theta \sin \theta}{(1 - \beta \cos \theta)^5} d\theta, \quad (1)$$

with

$$\tilde{R}(t) = \beta[c(t - t_c) - D] + R_c, \quad (2)$$

where D is the distance of the fireball to the observer, θ the angle of a concerned differential surface of the fireball to the line of sight, ν the observation frequency, $\nu_{0,\theta}$ the rest frame emission frequency of the differential surface, t_c a constant, which can be any coordinate time concerned, R_c the radius of the fireball at time t_c , $g_{0,\nu}(\nu_{0,\theta})$ the dominant mechanism, and I_0 the constant intensity magnitude for the radiation of the differential surface in the rest frame. Frequencies $\nu_{0,\theta}$ and ν are related by the Doppler effect, which is $\nu = \nu_{0,\theta}/\Gamma(1 - \beta \cos \theta)$. The proper time $t_{0,\theta}$ and observation time t can be well linked by considering the travelling of light from the fireball to the observer.

In this paper we consider the Band spectrum (Band et al. 1993) as the rest frame radiation (note in fact it is not a real radiation mechanism for the GRBs, perhaps it is the composition of some mechanisms (synchrotron, Comptonized mechanisms, etc.)), which is

$$g_{0,\nu,G}(\nu_{0,\theta}) = \begin{cases} \left(\frac{\nu_{0,\theta}}{\nu_{0,p}}\right)^{1+\alpha_{0,G}} \exp[-(2 + \alpha_{0,G})\frac{\nu_{0,\theta}}{\nu_{0,p}}] & \left(\frac{\nu_{0,\theta}}{\nu_{0,p}} < \frac{\alpha_{0,G} - \beta_{0,G}}{2 + \alpha_{0,G}}\right), \\ \left(\frac{\alpha_{0,G} - \beta_{0,G}}{2 + \alpha_{0,G}}\right)^{(\alpha_{0,G} - \beta_{0,G})} \exp(\beta_{0,G} - \alpha_{0,G}) \left(\frac{\nu_{0,\theta}}{\nu_{0,p}}\right)^{1+\beta_{0,G}} & \left(\frac{\nu_{0,\theta}}{\nu_{0,p}} \geq \frac{\alpha_{0,G} - \beta_{0,G}}{2 + \alpha_{0,G}}\right), \end{cases} \quad (3)$$

where $\alpha_{0,G}$ and $\beta_{0,G}$ are the lower and higher spectral indexes, respectively. In this work, we used the typical values: $\alpha_{0,G} = -1$ and $\beta_{0,G} = -2.25$ (Preece et al. 1998, 2000).

In Eq. (1) when the upper limit is $\pi/2$, the calculated spectrum represent the expected spectrum arising from the spherical fireball. We replaced the upper limit with the opening angle of the $1/\Gamma$ region and a uniform jet, respectively. For the uniform jet, we consider three cases: the smallest θ_{jet} (0.056), the biggest θ_{jet} (0.4) available, and their mean (0.228).

As the cosmological effect is small compared to Doppler effect in the gamma-ray bursts fireball framework, it can be ignored in our work. The rest frame radiation is assumed to be constant and independent of direction.

We calculated the expected spectra from the $1/\Gamma$ region, the spherical fireball and the uniform jets for four Lorentz factors, 1, 10, 100 and 500. The results are presented in Figure 1. When $\Gamma = 1$ they can clearly be distinguished. When $\Gamma = 10$, we find that only the spectrum of the jet with $\theta_{\text{jet}}=0.056$ can be told apart from the other spectra, while the other lines are superposed on one another. When $\Gamma = 100$ and 500, all merge into one and can not be distinguished. These results indicate that, in the prompt emission phase, when the Doppler factor is bigger, the observed spectra from the $1/\Gamma$ region, the spherical fireball and the uniform jet are similar with no obvious differences. At the same time, we also obtained that due to the Doppler effect for the spherical fireball or a uniform jet the observed radiation mainly comes from the $1/\Gamma$ region.

In order to further examine the differences among the expected spectra, we calculate the relative deviations (Δ),

$$\Delta = \frac{\nu f_\nu(t)_1 - \nu f_\nu(t)_2}{\nu f_\nu(t)_1}, \quad (4)$$

where suffix 1 refers to the spherical fireball and suffix 2, the $1/\Gamma$ region or the uniform jet with different opening angles. The results are presented in Figure 2.

In the $\Gamma = 1$ panel of Figure 2, the different lines from top to bottom are the relative deviation curves of the spherical fireball from the uniform jets with $\theta_{\text{jet}} = 0.056, 0.228$ and 0.4, and the $1/\Gamma$ region, respectively, and they are well separated. In the $\Gamma = 10$ panel, the top line is the relative deviation curve (always of the spherical fireball) from the uniform jet with $\theta_{\text{jet}} = 0.056$; the middle line is the relative deviation curve from the $1/\Gamma$ region; the bottom line is the superposed relative deviation from the uniform jets with $\theta_{\text{jet}} = 0.228$ and 0.4. In the $\Gamma = 100$ and 500 panels, there are just two lines: The bottom line is superposed relative deviation curve of the spherical fireball from the uniform jets, and except for some negligible vibrations around the peak energy, it almost keeps

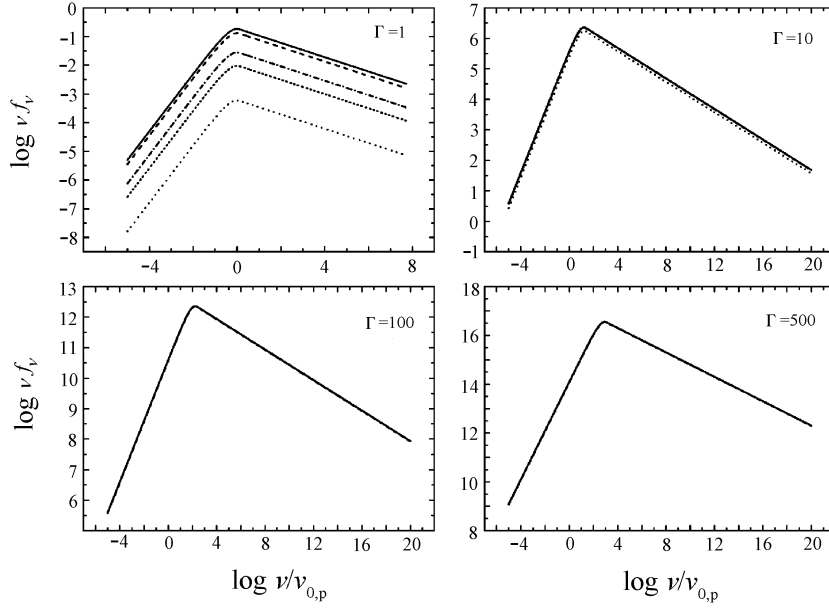


Fig. 1 Expected spectra from the $1/\Gamma$ region. The spherical fireball and the uniform jet are with $\theta_{\text{jet}} = 0.056, 0.228$ and 0.4 , respectively, where we take $2\pi I_0 \tilde{R}^2(t) \nu_{0,p}/D^2 = 1$. The dash lines are the expected spectra of the $1/\Gamma$ region. The solid lines are the expected spectra of the spherical fireball. The dot, dash dot and short dash lines represent the expected spectra from the uniform jet with $\theta_{\text{jet}} = 0.056, 0.4$ and 0.228 , respectively. When $\Gamma = 100$ and 500 , all the lines are superposed on one another and can not be distinguished.

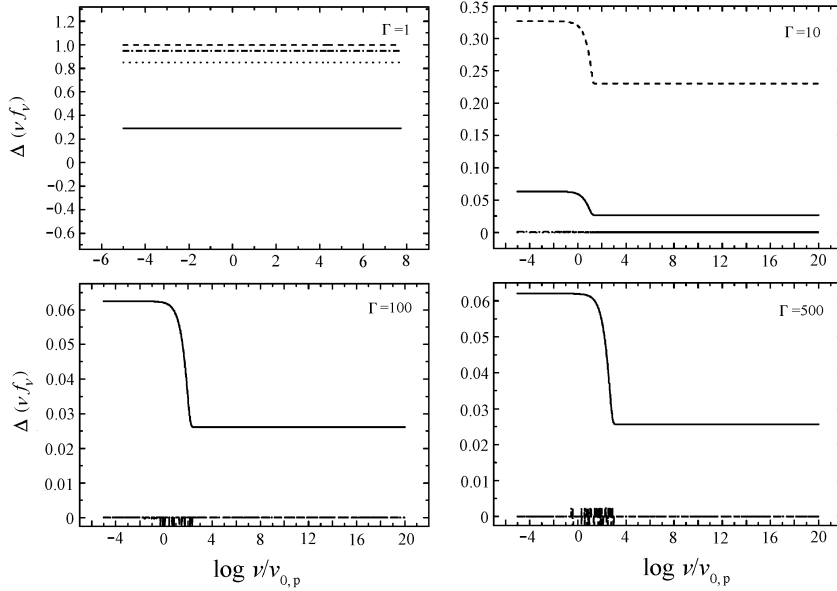


Fig. 2 Expected spectral relative deviations of the spherical fireball with the $1/\Gamma$ region and the uniform jets. The solid, dash, dash dot and dot lines represent the relative deviations of the spherical fireball from the $1/\Gamma$ region, and the jets with $\theta_{\text{jet}} = 0.056, 0.228$ and 0.4 , respectively. The relative deviation lines of the uniform jets and the spherical fireball are indistinguishable when $\Gamma = 100$ and 500 .

to the value 0. This strongly suggests that when Γ is large, the spectra for the spherical fireball and the uniform jet are same. The top line (with a break) is the relative deviation curve of the spherical fireball from the $1/\Gamma$ region. For $\Gamma = 10, 100, 500$, this curve first keeps to a fixed value, then falls monotonically and quickly to a minimum, and keeps to the minimum value to the end. The sharp drop appears in a range near the peak frequency, indicating that the peak frequency is a key frequency for the $1/\Gamma$ region, the spherical fireball and the uniform jet, which divides the frequency into low frequency range and high frequency range. For different frequency ranges, the relative deviation between the $1/\Gamma$ region and the spherical fireball is different, being bigger in the low than in the high frequency range, indicating that the role of the $1/\Gamma$ region is different in different frequencies, that radiation from the $1/\Gamma$ region is larger in the high than in the low frequencies.

3 THE EXPECTED EMISSION LINES

In this section we examine the expected emission lines from the $1/\Gamma$ region, the spherical fireball and the uniform jets. Radiation in the rest frame was described to be of the form,

$$g_{0,\nu}(\nu_{0,\theta}) = \max\{g_{0,\nu,G(\nu_{0,\theta})} + \sum_{i=1}^n e_{0,\nu,i(\nu_{0,\theta})}, 0\}, \quad (5)$$

where $e_{0,\nu,i(\nu_{0,\theta})}$ describes the relative intensity of lines:

$$e_{0,\nu,i(\nu_{0,\theta})} = \frac{h_i}{\exp(2 + a_0)} \exp\left[-\frac{(\nu_{0,\theta}/\nu_{0,p} - \nu_{0,\text{line},i}/\nu_{0,p})^2}{(2 \times 10^{n_i})}\right]. \quad (6)$$

Here we followed Qin (2003) and considered two narrow emission lines,

$$\nu_{0,\text{line},1}/\nu_{0,p} = 0.01, \quad h_1 = 1000, \quad n_1 = -8, \quad (7)$$

and

$$\nu_{0,\text{line},2}/\nu_{0,p} = 100, \quad h_2 = 1, \quad n_2 = 0. \quad (8)$$

The results of the expected emission lines from the $1/\Gamma$ region, the spherical fireball and the uniform jets are shown in Figure 3.

From Figure 3 we find when $\Gamma = 1$, the emission lines from the spherical fireball and the uniform jets are not broadened and the $1/\Gamma$ region can be clearly distinguished. When $\Gamma = 10, 100$ and 500 the emission lines from the $1/\Gamma$ region and the uniform jets are obviously broadened, and these emission lines also move to high frequency. This is consistent with the results of the spherical fireball obtained by Qin (2003). When $\Gamma = 100$ and 500, the emission lines from the uniform jets are the same as that from the spherical fireball, and they can not be distinguished. It is interesting that the emission lines from the $1/\Gamma$ region show a break at the beginning of the emission lines. A break also can be found for the uniform jet with the smallest opening angle when $\Gamma = 10$.

To show the broadening of the emission lines, we calculate the relative width of the $\Delta\nu_{\text{FWHM}}/\nu_{\text{line}}$, where ν_{line} is the observed line frequency at which the peak flux of the line feature is found. Listed in Table 1 are the values of ν_{line} and $\Delta\nu_{\text{FWHM}}/\nu_{\text{line}}$ of these two emission lines for various values of Γ for the uniform jets, the spherical fireball and the $1/\Gamma$ region in the Band spectrum. The relative width is 0.0246 in the rest frame (see the case of $\Gamma=1$ in Table 1). When the fireball expands relativistically, the relative width approaches the same asymptotic value (0.171) for the uniform jets, the spherical fireball and the $1/\Gamma$ region. Thus, it is impossible to use the relative width to tell them apart. Finally, we may note that the curvature effect shows up in the broadening of the emission lines, and the Doppler effect, in the shifted frequency and the enhanced flux.

4 THE EXPECTED PULSE PROFILES

Some simple bursts with well-separated features suggest that they may consist of fundamental units of radiation or pulses, with some of them showing a fast rise and an exponential decay

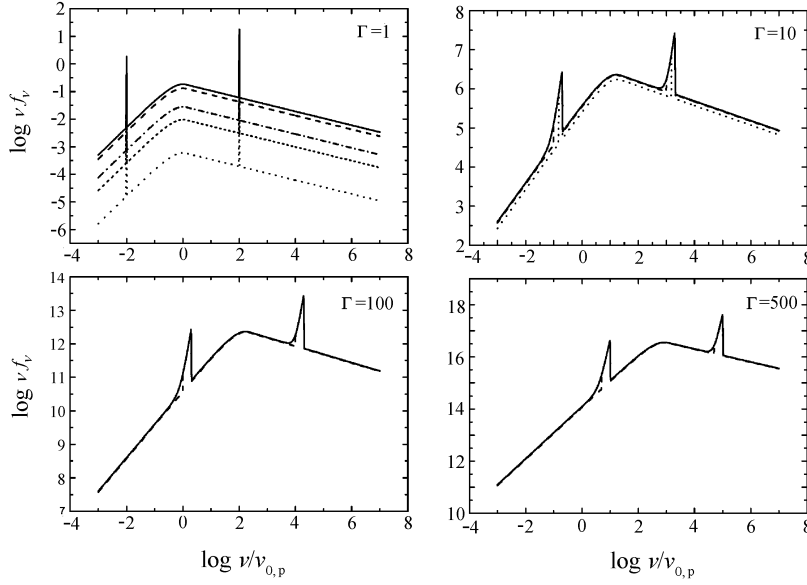


Fig. 3 Expected spectrum plus the two emission lines defined by Eqs.(7) and (8), from the $1/\Gamma$ region, the spherical fireball and the uniform jets, respectively, and we have taken $2\pi I_0 \tilde{R}^2(t) \nu_{0,p}/D^2 = 1$. The dash, solid, dot, dash dot and short dash lines represent expected spectrum plus the two emission lines from the $1/\Gamma$ region, the spherical fireball and the uniform jet with $\theta_{\text{jet}} = 0.056, 0.4$ and 0.228 , respectively. When $\Gamma = 100, 500$, all the lines are superposed on one another and can not be distinguished.

(FRED) phase (Fishman et al. 1994). These FRED pulses could be well represented by a flexible empirical function, and with this empirical function many statistical properties of pulses of GRBs were revealed (Norris et al. 1996). Recently, light curves with FRED pulses were interpreted as signatures of the relativistic curvature effect (the Doppler effect over the fireball surface) (Fenimore et al. 1996; Ryde & Petrosian 2002; Kocevski et al. 2003; Qin et al. 2004). In this section we used the formula obtained by Qin et al. (2004) to investigate the difference of the pulse of the light curves between the spherical fireball and the uniform jets. Here we adopted eq. 21 of Qin et al. (2004) to calculate the count rate, namely,

$$C(\tau) = \frac{2\pi R_c^3 \int_{\tilde{\tau}_{\theta,\min}}^{\tilde{\tau}_{\theta,\max}} \tilde{I}(\tau_{\theta})(1 + \beta\tau_{\theta})^2(1 - \tau + \tau_{\theta})d\tau_{\theta} \int_{v_1}^{v_2} \frac{g_{0,\nu}(\nu_{0,\theta})}{\nu} d\nu}{hcD^2\Gamma^3(1 - \beta)^2(1 + k\tau)^2}, \quad (9)$$

where h is the Plank constant, and k , τ , $\tilde{\tau}_{\theta,\max}$ and $\tilde{\tau}_{\theta,\min}$ are determined by

$$k \equiv \frac{\beta}{1 - \beta}, \quad (10)$$

$$\tau_{\theta} = \frac{\tau - (1 - \cos\theta)}{1 - \beta \cos\theta}, \quad (11)$$

$$\tilde{\tau}_{\theta,\max} = \min(\tau_{\theta,\max}, \frac{\tau - 1 + \cos\theta_{\min}}{1 - \beta \cos\theta_{\min}}), \quad (12)$$

$$\tilde{\tau}_{\theta,\min} = \max(\tau_{\theta,\min}, \frac{\tau - 1 + \cos\theta_{\max}}{1 - \beta \cos\theta_{\max}}), \quad (13)$$

respectively. Here we used the Band function (Eq.(4)) as the local radiation and a local rectangle pulse (eq.(56) of Qin et al. (2004)) to examine this issue. The rectangular pulse is described by

$$\tilde{I}(\tau_{\theta}) = \begin{cases} I_0, & \tau_{\theta,\min} \leq \tau_{\theta} \leq \tau_{\theta,\max}, \\ 0, & \tau_{\theta,\min} > \tau_{\theta}, \tau_{\theta} > \tau_{\theta,\max}. \end{cases} \quad (14)$$

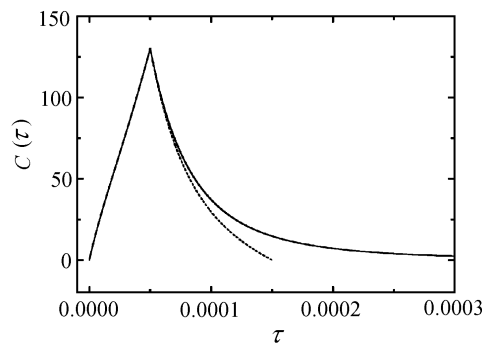


Fig. 4 Expected pulse from the $1/\Gamma$ region, the uniform jets and the spherical fireball, where we take $\Gamma=100$, $\tau_{\theta,\min} = 0$, $\tau_{\theta,\max} = 1.0$, $v_1 = 110$ keV, $v_2 = 320$ keV. The pulses of spherical fireball, and the uniform jet with $\theta_{\text{jet}} = 0.056, 0.4$ and 0.228 , are represented by the solid line. The dash line represents the pulse of the $1/\Gamma$ region.

We take $\Gamma=100$, $\tau_{\theta,\min} = 0$, $\tau_{\theta,\max} = 1.0$, $v_1 = 110$ keV, $v_2 = 320$ keV, and the results are presented in Figure 4.

As the pulses from the uniform jets and the spherical fireball are superposable and can not be told apart, the solid line is used. This suggests that for the light curves in prompt emission phase there is no obvious difference between the spherical fireball and the uniform jet. This means we cannot use the light curves of the GRBs to discern whether it originates from a spherical fireball or a uniform jet. From Figure 4 the pulse from the $1/\Gamma$ region and the spherical fireball are superposable in the rise phase and it is clearly separated at the drop phase. In the drop phase we find the pulse of the $1/\Gamma$ region is below the pulse of the fireball and uniform jets.

5 DISCUSSION AND CONCLUSIONS

Under the consideration of the Doppler effect we have investigated the different features, including the spectra, emission lines and profiles of pulse, of uniform jets, $1/\Gamma$ region and isotropic fireballs in the gamma-ray burst phase.

When the Lorentz factors is large (say $\Gamma > 10$), the spectra, the emission lines and the pulse profiles are the same for a uniform jet and an isotropic fireball. However, Figure 2 also shows that the relative deviation between the two is not zero around the spectral peak. After a test it has been verified that this is due to the imprecision of the integral and relative deviation would vanish with improved integration. Thus, the uniform jets and the isotropic fireball present the same spectral characteristics and in the Gamma-ray burst phase we cannot tell whether the GRB comes from a uniform jet or an isotropic fireball.

The spectra, emission lines and pulse profiles of the $1/\Gamma$ region are not same as those of the isotropic fireball: there are some small differences. For example, the relative deviations of the spectra are not zero, the broadened emission lines show a break at a low frequency, and the profile of the pulse is below that of the isotropic fireball in the drop phase. However, we also find these differences to be not so important: first, when $\Gamma > 10$ the spectra of the $1/\Gamma$ region and the isotropic fireball are almost superposable: the former is no less than 93% of the latter in the lower frequencies and not less than 97% in the higher frequencies; secondly, the FWHM of the broadened emission lines of the $1/\Gamma$ region is the same as that of the isotropic fireball; thirdly, the shape of the pulse profiles of the $1/\Gamma$ region and the isotropic fireball are similar. This means, due to the relativistic beaming effect, the $1/\Gamma$ region plays a leading role in these features of the isotropic fireball. This is also the reason that the uniform jet and the isotropic fireball show the same characters in these aspects.

Finally, we can draw conclusions as follows: (1) Due to the relativistic beaming effect, the spectra, emission lines and pulse profiles of the spherical fireball or a uniform jet mostly come from the $1/\Gamma$ region. So we can use the $1/\Gamma$ region to substitute the isotropic fireball or the uniform jet in approximate calculations. (2) Since the uniform jet and the isotropic fireball can not be

distinguished in these observed features, we must resort to further means to resolve the issue whether the GRB in the prompt emission phase arises from a spherical fireball or a uniform jet. (3) Emission line broadening is a general phenomena, which mainly comes from the curvature effect. (4) The role played by the $1/\Gamma$ region is different in different frequencies: the radiation from the $1/\Gamma$ region is stronger in the higher than lower frequencies.

Acknowledgements We would like to thank the anonymous referee for his or her several incisive and substantive comments and suggestions, which have allowed us to improve this revised paper greatly. This work was supported by the Special Funds for Major State Basic Research Projects (“973”) and the National Natural Science Foundation of China (Grant 10273019).

References

- Band D., Matteson J., Ford L. et al., 1993, *ApJ*, 413, 281
 Berger E., Kulkarni S. R., Pooley G. et al., 2003, *Nature*, 426, 154
 Bloom J. S., Frail D. A., Kulkarni S. R., 2003, *ApJ*, 594, 674
 Cheng K. S., Lu T., 2001, *ChJAA*, 1, 1
 Dado S., Dar A., De Rujula A., 2002a, *ApJ*, 572, L143
 Dado S., Dar A., De Rujula A., 2002b, *A&A*, 388, 1079
 Dai Z. G., Cheng K. S., 2001, *ApJ*, 558, 109
 Dai Z. G., Huang Y. F., Lu T., 2001, *MNRAS*, 324, L11
 Eriksen E., Gron O., 2000, *Amer. J. Phys.*, 68, 1123
 Fenimore E. E., Madras C.D., Nayakshin S., 1996, *ApJ*, 473, 998
 Fishman G. J., Meegan C. A., Wilson R. B. et al., 1994, *ApJS*, 92, 229
 Frail D. A., Kulkarni S. R., Sari R. et al., 2001, *ApJ*, 562, L55
 Friedman A. S., Bloom J. S., 2005, *ApJ*, 627, 1
 Goodman J., 1986, *ApJ*, 308, L47
 Granot J., Piran T., Sari R., 1999, *ApJ*, 513, 679
 Huang Y. F., Tan C. Y., Dai Z. G., et al. 2002, *Chin. Astron. Astrophys.*, 26, 414
 Huang Y. F., Wu X. F., Dai Z. G. et al., 2004, *ApJ*, 605, 300
 Kocevski D., Pyde F., Liang E., 2003, *ApJ*, 596, 389
 Mészáros P., 2002, *ARA&A*, 40, 137
 Mészáros P., Rees M. J., 1998, *ApJ*, 502, L105
 Paczyński B., 1986, *ApJ*, 308, L43
 Panaitescu A., Mészáros P., Rees M. J., 1998, *ApJ*, 503, 314
 Norris J. P., Nemiroff R. J., Bonnell J. T. et al., 1996, *ApJ*, 459, 393
 Panaitescu A., Kumar P., 2001, *ApJ*, 560, L49
 Piran T., 1999, *Physics Reports*, 314, 575
 Piran T., 2005, *Reviews of Modern Physics*, 76, 1143
 Preece R. D., Briggs M. S., Malozzi R. S. et al., 2000, *ApJS*, 126, 19
 Preece R. D., Pendleton G. N., Briggs M. S. et al., 1998, *ApJ*, 496, 849
 Qin Y.-P., 2003, *A&A*, 407, 393
 Qin Y.-P., 2002, *A&A*, 396, 705
 Qin Y.-P., Zhang, Z.-B., Zhang, F.-W. et al., 2004, *ApJ*, 617, 439
 Rhoads J. E., 1997, *ApJ*, 487, L1
 Rhoads J. E., 1999, *ApJ*, 525, 737
 Rossi E., Lazzati D. Rees M.J., 2002, *MNRAS*, 332, 945
 Ryde F., Petrosian V., 2002, *ApJ*, 578, 290
 Sari R., Piran T. Halpern J. P., 1999, *ApJ*, 519, L17
 Sari R. Piran T., 1999, *ApJ*, 517, L109
 Waxman E., Kulkarni S. R. Frail D. A., 1998, *ApJ*, 497, 288
 Wei D. M., Jin, Z. P., 2003, *A&A*, 400, 415
 Zhang B., Mészáros P., 2002, *ApJ*, 571, 876
 Zhang B., Mészáros, P., 2004, *International Journal of Modern Physics A*, 19, 2385
 Zhang B., Kobayashi S. Mészáros P., 2003, *ApJ*, 595, 950